Atomic crystal structure of ordered In3Sb1Te2 ternary alloy studied by high-resolution transmission electron microscopy

Chung Soo Kim, Jeong Yong Lee, and Yong Tae Kim

Citation: Appl. Phys. Lett. **100**, 151903 (2012); doi: 10.1063/1.3702575
View online: http://dx.doi.org/10.1063/1.3702575
View Table of Contents: http://apl.aip.org/resource/1/APPLAB/v100/i15
Published by the American Institute of Physics.

Atomic crystal structure of ordered $In_3Sb_1Te_2$ ternary alloy studied by high-resolution transmission electron microscopy

Chung Soo Kim,[1] Jeong Yong Lee,[1,a)] and Yong Tae Kim[2,b)]
[1]*Department of Materials Science and Engineering, KAIST, Daejeon 305-701, Korea*
[2]*Semiconductor Materials and Devices Laboratory, Korea Institute of Science and Technology (KIST), Seoul 130-650, Korea*

(Received 22 November 2011; accepted 23 March 2012; published online 10 April 2012)

The atomic structure of $In_3Sb_1Te_2$ was investigated by high-resolution transmission electron microscopy (HRTEM) and the National Center for Electron Microscopy Simulation System. $In_3Sb_1Te_2$ has a disordered NaCl structure; In atoms are positioned in a face-centered cubic lattice, and Sb and Te atoms are located at randomly occupied octahedral sites. However, the observed HRTEM images of the ordered $In_3Sb_1Te_2$ phase show that Sb and Te atoms are located in specific positions, that is, at the center and edge of the unit cell, respectively. The atomic model of the ordered $In_3Sb_1Te_2$ is confirmed by simulated images, which match the experimental HRTEM images. © *2012 American Institute of Physics*. [http://dx.doi.org/10.1063/1.3702575]

Phase change random access memory (PRAM) based on chalcogenide alloys has attracted much attention for next generation non-volatile memory due to its fast operation, high scalability, and low fabrication costs.[1] A remarkable characteristic of PRAM materials is a reversible phase transformation, which has different electrical properties between amorphous and crystalline phases. That is, the amorphous state has a relatively high resistivity, whereas the crystalline state has a low resistivity. Among the chalcogenide materials, Ge-Sb-Te (GST) is well known as a recording material in phase change memory devices because of its fast speed of transformation and the good stability of the amorphous phase. In spite of these advantages, there is increasing demand for an improvement in power consumption and storage density.[2,3] To solve these issues, many researchers have focused on other chalcogenide materials such as Si-Sb-Te,[4] Ga-Sb-Te,[5] and Al-Sb-Te.[6] From this point of view, we investigated the In-Sb-Te (IST) material for PRAM application. IST is already known as an optical data storage material, and the optical and electrical properties have been reported.[7–9] In a previous paper, the IST phase change material had four different resistance states for multi-bit storage in PRAM.[10] The respective phases corresponding to multilevel states were also confirmed. However, a high-resolution transmission electron microscopy (HRTEM) study on an atomic level was little investigated for the crystal structure and atomic arrangement of IST material. Furthermore, it is important to understand the microstructure of IST for phase change performance which is phase transformation behavior and nucleation-growth mechanism. In this letter, we demonstrate the crystal structure of the $In_3Sb_1Te_2$ ternary alloy through combined studies using HRTEM and the computer simulation system.

An IST thin film with a thickness of 200 nm was deposited by RF magnetron sputtering on a SiO_2/Si(001) substrate. The sputtering was carried out with a 3-in. $In_3Sb_1Te_2$ single target (99.99%) in an Ar ambient, and the deposition rate was 40 nm/min at 40 W. The rapid thermal annealing (RTA) process was carried out at 450 °C for 10 and 60 min in a N_2 ambient condition, respectively. The TEM specimens were prepared by mechanical polishing, followed by Ar ion milling together with liquid nitrogen cooling to prevent crystallization due to sample heating. Ion milling was performed under the conditions of 4 kV and 0.4 mA with Ion Mill Model 1010 (Fischione Instruments). For the bright-field transmission electron microscopy (BFTEM) images, selected area electron diffraction (SAED) patterns, and HRTEM images, we used a 300 kV TEM (Jeol JEM-3010) equipped with a CCD camera (Gatan USC4000). Simulated images of the atomic arrangement were also obtained using the National Center for Electron Microscopy Simulation System (NCEMSS) of the Lawrence Berkeley National Laboratory.

Figure 1 shows the cross-sectional BFTEM image, SAED pattern, and HRTEM image of the IST thin film annealed at 450 °C for 10 min. The thin film is polycrystalline, with randomly oriented grains in the approximate size range 10–50 nm, as shown in Fig. 1(a). From the SAED analysis shown in Fig. 1(b), the grains are in the $In_3Sb_1Te_2$ phase, which has the NaCl structure with a unit cell

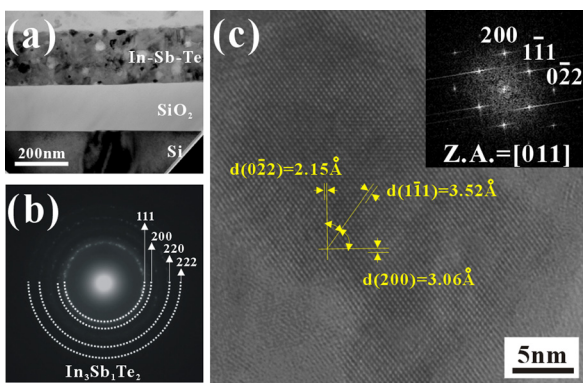

FIG. 1. (a) BFTEM image and (b) SAED pattern of the IST thin film annealed at 450 °C for 10 min. (c) HRTEM image and FFT pattern (inset) of the disordered $In_3Sb_1Te_2$ ternary alloy.

a)Electronic mail: j.y.lee@kaist.ac.kr.
b)Electronic mail: ytkim@kist.re.kr.

parameter $a_0 = 6.12$ Å. The $In_3Sb_1Te_2$ ternary alloy consists of In atoms in face-centered cubic (fcc) sites and Sb and Te atoms occupying the octahedral sites, respectively.[11] The HRTEM image and corresponding fast Fourier transform (FFT) pattern of the $In_3Sb_1Te_2$ phase are shown in Fig. 1(c). Along the [011] zone axis, the lattice contrast of the HRTEM image should be uniform for all atomic sites. Because the Sb and Te atoms occupy the same atomic positions, the HRTEM and the FFT pattern (inset) indicate that a superlattice phase does not exist. In addition, it was reported that the superlattice structure was not observed in $In_3Sb_1Te_2$ nanowires synthesized by a metal-organic chemical vapor deposition (MOCVD).[12] The nanowires were grown at a low temperature of 250 °C and high working pressures of 13×10^2 Pa. From the TEM analysis, it was confirmed that the crystal structure of the nanowires was consistent with the structure of the IST thin film annealed at 450 °C for 10 min. Therefore, we conclude that $In_3Sb_1Te_2$ assumes the disordered NaCl structure like metastable GST.[13]

Figure 2(a) shows a BFTEM image of an IST thin film annealed at 450 °C for 60 min. The $In_3Sb_1Te_2$ grains in the film are 50–100 nm in size. Figures 2(b) and 2(d) show BFTEM images of the edge region of the thin film. The corresponding SAED patterns are observed along the directions of the [011] and [012] zone axes as shown in Figs. 2(c) and 2(e), respectively. One of the most interesting findings in this experiment is the extra spots, which are marked with yellow color in the figures (100, $0\bar{1}1$, $2\bar{2}1$, $1\bar{2}1$, $0\bar{2}1$, and so on). The original diffraction spots in the $In_3Sb_1Te_2$ ternary alloy are $1\bar{1}1$, 200, $0\bar{2}2$, and so on. Compared with the FFT pattern along the [011] zone axis, the 100 and $0\bar{1}1$ spots should not be found in the NaCl structure of the $In_3Sb_1Te_2$ phase, as shown in the inset of Fig. 1(c). Generally, reflections possibly present, but their intensity is different, if h, k, and l which are the Miller indices of a plane are unmixed. Thus, reflections occur for such planes as (111), (200), and (220) but not for the planes (100), (011), (021), and so on in the $In_3Sb_1Te_2$ phase. From this result, it is clear that the atomic structure of $In_3Sb_1Te_2$ has a periodical arrangement of Sb and Te atoms, because for an ordered material there will be superlattice reflections at the positions which are forbidden for the disordered structure.

To reveal more structural details of the $In_3Sb_1Te_2$ crystal, we present HRTEM images along the [011] and [012] directions in Figs. 3(a) and 3(b), respectively. The HRTEM images show the different lattice contrast with an array of bright and dark lines that come from the superlattice reflections. Extra diffraction spots are also observed in the FFT images of the insets. The crystal structure appears to possess a certain periodic relationship between Sb and Te atoms. We suppose that In atoms are not changed in the fcc sites, whereas Sb and Te atoms are located at specific positions among the octahedral sites. The interplanar spacing of (200) is 3.06 Å, which is the same as for the disordered crystalline phase of $In_3Sb_1Te_2$, but the distance of the (100) plane increases to 6.12 Å, which is double the spacing of the (200) plane, without a change in lattice parameter. The atomic arrangements along the [011] and [012] zone axes are illustrated in Figs. 3(c) and 3(d), respectively. In the [011] projection of the disordered $In_3Sb_1Te_2$ structure, Sb and Te

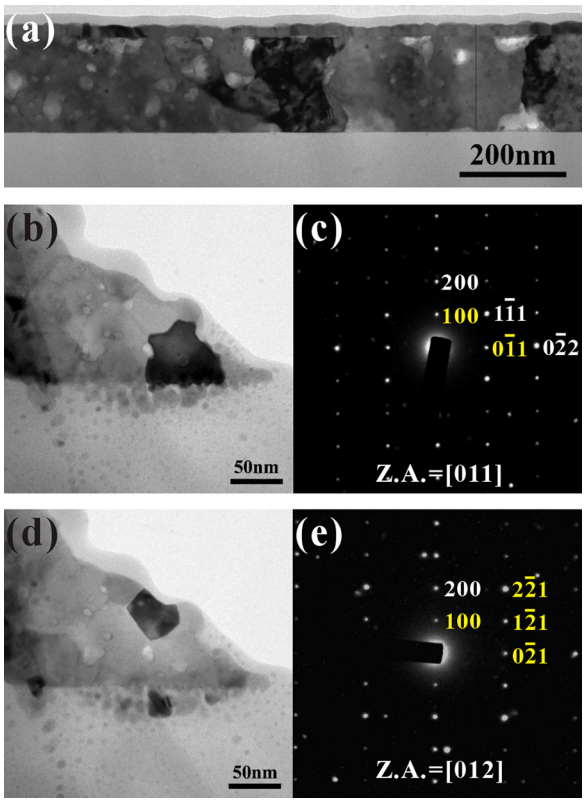

FIG. 2. (a) BFTEM image of the IST thin film annealed at 450 °C for 60 min. (b), (d) BFTEM images of the edge region of the thin film. (c), (e) Corresponding SAED patterns of (b) and (d), respectively. The original diffraction spots of the NaCl structure are represented by white characters, and extra spots are yellow characters.

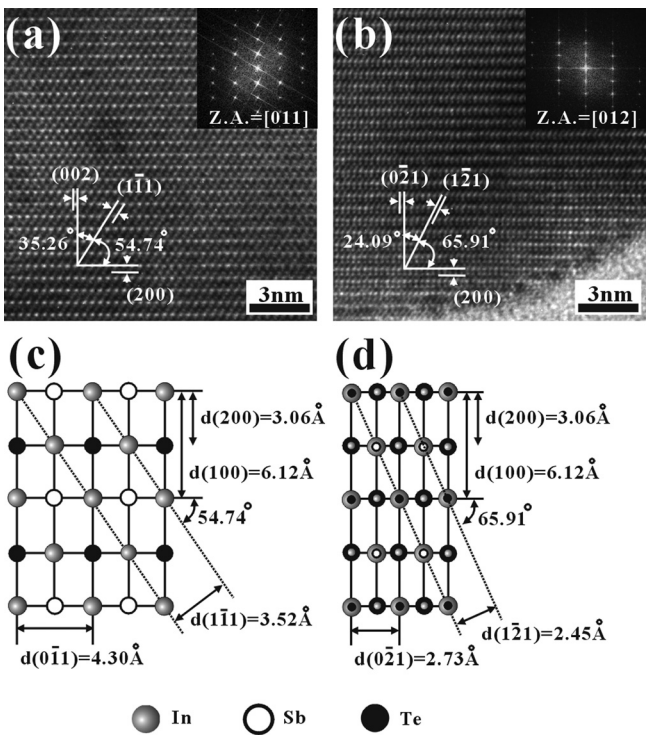

FIG. 3. (a), (b) Experimental HRTEM images of the ordered $In_3Sb_1Te_2$ observed on the direction of [011] and [012] zone axes, respectively. (c), (d) Schematic illustrations of the ordered $In_3Sb_1Te_2$ atomic arrangement on the (011) and (012) planes.

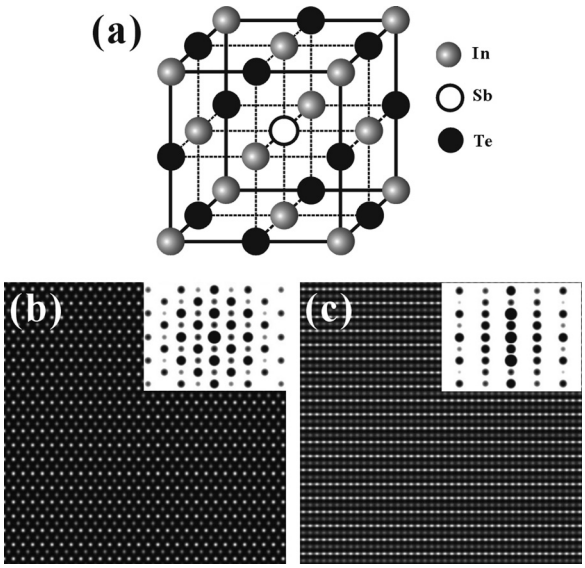

FIG. 4. (a) 3-dimensional atomic structure model of the ordered $In_3Sb_1Te_2$ ternary alloy. (b), (c) Simulated HRTEM images of the ordered $In_3Sb_1Te_2$ viewed along [011] and [012] directions, respectively. They are well matched with experimental HRTEM images of Figs. 3(a) and 3(b).

atoms overlap each other randomly. However, the (100) and (200) planes are occupied with the different stacking sequence in the ordered $In_3Sb_1Te_2$ phase, as shown in Fig. 3(c). The contrast difference in the HRTEM image occurs due to the stacking sequence of -Te-Te- or -Te-Sb-. We also present the atomic arrangement of the [012] zone axis in Fig. 3(d). The atomic sequences in the [012] direction are -In-Te- and -In-Sb-.

The atomic structure model of ordered $In_3Sb_1Te_2$ is described in Fig. 4(a). The construction is based on the atomic arrangements along the [011] and [012] directions, as shown in Figs. 3(c) and 3(d), respectively. While In atoms occupy a fcc lattice, Sb and Te atoms are located at the center and edge of the unit cell, respectively. In order to verify the atomic structure of the ordered $In_3Sb_1Te_2$, simulations of the HRTEM image and SAED patterns were performed using the NCEMSS software. We carried out the HRTEM simulations as a function of defocus and thickness based on the model, as shown in Fig. 4(a). Figures 4(b) and 4(c) show the simulated HRTEM images and corresponding electron diffraction patterns, respectively. The simulated HRTEM image was obtained using a defocus of 44 nm, a thickness of 10 nm, and the [011] zone axis, as shown in Fig. 4(b), and the results are consistent with the experimental HRTEM image shown in Fig. 3(a). Similarly, Fig. 4(c) shows the simulated HRTEM image along the [012] beam direction using a defocus of 55 nm and a thickness of 25 nm. It also matches the observed HRTEM images well, as shown in Fig. 3(b).

In summary, we have investigated to understand the atomic structure of the $In_3Sb_1Te_2$ ternary alloy using HRTEM and NCEMSS. According to the different annealing times, disordered and ordered $In_3Sb_1Te_2$ phases are observed. The disordered $In_3Sb_1Te_2$ has the NaCl structure which consists of Sb and Te atoms randomly occupying the octahedral sites, whereas the ordered $In_3Sb_1Te_2$ has Sb and Te atoms located at the center and edge of the unit cell, respectively. The 3-dimensional atomic structure model of the ordered $In_3Sb_1Te_2$ phase is confirmed by experimental and simulated HRTEM images along the [011] and [012] zone axes. These results provide a fundamental understanding of the IST chalcogenide material for multilevel PRAM.

This work was supported by R&D Program of the Ministry of Knowledge Economy (The next generation MLC PRAM, 3-dimensional ReRAM, Device Material and Micro Fabrication Technology Development).

[1]M. H. R. Lankhorst, B. W. S. M. M. Ketelaars, and R. A. M. Wolters, Nat. Mater. **4**, 347 (2005).
[2]M. Wuttig and N. Yamada, Nat. Mater. **6**, 824 (2007).
[3]S. Raoux, W. Welnic, and D. Ielmini, Chem. Rev. **110**, 240 (2010).
[4]X. Zhou, L. Wu, Z. Song, F. Rao, Y. Cheng, C. Peng, D. Yao, S. Song, B. Liu, S. Feng, and B. Chen, Appl. Phys. Lett. **99**, 032105 (2011).
[5]H.-Y. Cheng, S. Raoux, and J. L. Jordan-Sweet, Appl. Phys. Lett. **98**, 121911 (2011).
[6]C. Peng, Z. Song, F. Rao, L. Wu, M. Zhu, H. Song, B. Liu, X. Zhou, D. Yao, P. Yang, and J. Chu, Appl. Phys. Lett. **99**, 043105 (2011).
[7]K. D. Flynn and D. Strand, Jpn. J. Appl. Phys. **42**, 795 (2003).
[8]Y. Maeda, H. Andoh, I., Ikuta, and H. Minemura, J. Appl. Phys. **64**, 1715 (1988).
[9]V. A. Kulbachinskii, Z. M. Dasshevskii, M. Inoue, M. Sasaki, H. Negishi, W. X. Geo, P. Lostak, J. Horak, and A. de Visser, Phys. Rev. B **52**, 10915 (1995).
[10]Y. I. Kim, E. T. Kim, J. Y. Lee, and Y. T. Kim, Appl. Phys. Lett. **98**, 091915 (2011).
[11]K. Deneke and A. Rabenau, Z. anorg. allgem. Chem. **333**, 201 (1964).
[12]J.-K. Ahn, K.-W. Park, H.-J. Jung, and S.-G. Yoon, Nano Lett. **10**, 472 (2009).
[13]A.V. Kolobov, P. Fons, A.I. Frenkel, A. L. Ankudinov, J. Tominga, and T. Uruga, Nat. Mater. **3**, 703 (2004).